THE PENNSYLVANIA STATE UNIVERSITY
SCHREYER HONORS COLLEGE

DEPARTMENT OF VETERINARY AND BIOMEDICAL SCIENCES

CHARACTERIZING THE ROLE OF IRE1α IN EARLY STAGES OF UVB INDUCED NEOPLASTIC TRANSFORMATION

STEPHEN D. WORRELL
SPRING 2020

A thesis
submitted in partial fulfillment
of the requirements
for a baccalaureate degree in Immunology and Infectious Disease
with honors in Immunology and Infectious Disease

Reviewed and approved* by the following:

Adam Glick
Professor of Toxicology and Carcinogenesis
Thesis Supervisor

Pamela Hankey
Professor of Immunology
Honors Adviser

* Electronic approvals are on file.

ABSTRACT

The endoplasmic reticulum (ER) is a vital cell organelle with diverse function, however the primary function is protein production. This process is highly important and tightly regulated but, under different forms of environmental stimuli or disease, can become dysregulated. When proteins are produced improperly, they can accumulate to cause deleterious stress to the cell, termed ER stress. To mitigate this, cells initiate a process called the unfolded protein response (UPR). The three arms of the UPR are controlled by the proteins ATF-6, PERK, and IRE1α. This thesis will investigate the role of IRE1α in responding to acute and chronic UVB exposure.

IRE1α is an ER membrane-spanning protein with two main effector functions in response to ER stress. First, upon UPR activation, IRE1α splices the transcription factor XBP-1 into the active form so it can translocate to the nucleus and regulate gene expression of many different proteins. Second, IRE1α will begin to degrade mRNA transcripts to decrease the protein levels to prevent more improper protein folding. These processes can significantly influence a cell's response to environmental or disease induced stress.

One important environmental stress Humans face every day is ultra-violet (UV) light from the sun. UV is a known inducer of ER stress and is the primary cause of skin cancer. Here, we worked to characterize how epidermal IRE1α plays a role in responding to acute and chronic UV-B exposure, using a congenital epidermal IRE1α knock-out mouse model.

TABLE OF CONTENTS

LIST OF FIGURES

ACKNOWLEDGEMENTS

First and foremost, I would like to thank Dr. Adam Glick for his continued support and instrumental role in my college journey. He has a unique faith in undergraduate students to conduct and contribute to research in a way that fosters true learning. By allowing me to conduct research in his lab for nearly three years, he sparked a passion for scientific investigation within me that will last a lifetime. Additionally, I would like to thank my mentor and good friend, Jeongin Son. When I first began helping Jeongin with research, I knew very little about technical skills and background knowledge I would need. He took the time and energy to train me on numerous techniques that are demonstrated in this thesis. Jeongin was always patient and kind with me, even through countless mistakes. He also put up with my hectic schedule that often got in the way. I admire Jeongin's passion and work ethic when it comes to research, as he often works after everyone else in the lab has left. I will always be grateful to have such an amazing mentor and friend. Additionally, I want to thank previous and current lab members Jake Bailey, Daniel Han, Fiona Chalmers, Saie Mogre, Justyn DuSold, Lily Robinson, Rose Gogal, and Chase Minnich. They were all ready and willing to answers any questions I had, in addition to being amazing friends.

I also owe a great debt of gratitude to my friends and family. Through the long days and nights of managing a busy school schedule with lab work, I often needed words of encouragement from them. Specifically I want to thank my mom Sally, my dad Ted, my sister Mary Kate, and my brother Teddy. They gave me all the love and support to motivate me along the difficult road.

Chapter 1

Introduction

1.1 Overview

This introduction will serve to provide background information on the Endoplasmic Reticulum and associated stress responses. A particular emphasis will be on the role of IRE1α in this pathway, as it is a focal point of this thesis. Additionally, the role of ER stress in various forms of pathogenesis will be discussed, with an emphasis on disease induced by Ultraviolet-B (UVB) radiation. Overall, this thesis will serve to characterize important cellular processes related to ER stress, mediated by IRE1α, in the context of acute and chronic UVB exposure. Figure 1 below outlines the mechanisms that I will be investigating in this thesis.

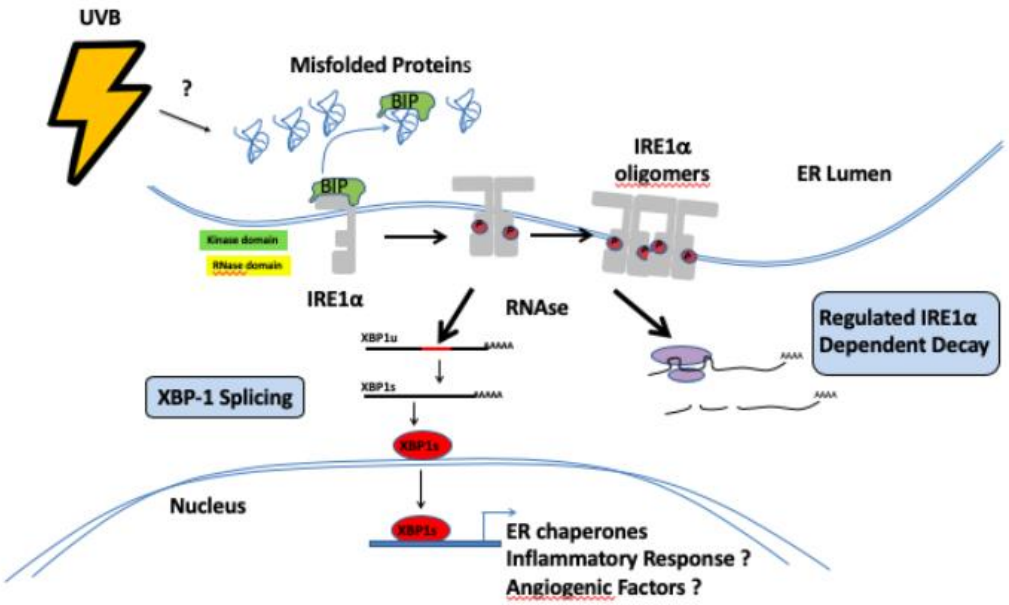

Figure 1: Schematic of IRE1α UPR pathway following ER stress

1.2 Endoplasmic Reticulum and ER Stress

The endoplasmic reticulum (ER) is the largest organelle in a cell and is dynamic, multifunctional, and intricate (1). In addition to functions like lipid synthesis and calcium storage, the ER is the primary site of protein folding (1). Once a polypeptide sequence has been completely synthesized and designated for the secretory pathway by a signal sequence, it will enter the lumen of the ER and begin a complex process called protein folding. As a vital site of protein folding, the majority of ER resident proteins are dedicated to proper protein folding, much like quality control on an assembly line (2). In the ER, protein folding related proteins called chaperones function to aid unfolded proteins into their correct conformations necessary for completing their physiological function (3). If proteins are not guided to reach their proper native conformations, various pathologies can result. Improper protein folding can result in diseases like metabolic disorders, inflammatory disease, and even cancer (4).

As a dynamic organelle, the ER must respond to environmental or internal cell stress. These stressors can perturb normal protein folding and modification, termed ER stress. In response to ER stress, cells have evolved a mechanism called the Unfolded Protein Response (UPR) to mitigate issues that arise from the presence of misfolded proteins (5). The first function of the UPR is to upregulate aforementioned molecular chaperones to promote proper protein folding or to fix misfolded proteins (6). Second, the UPR transiently slows protein translation to reduce the work burden of the ER (6). Finally, the UPR promotes the degradation of misfolded proteins, again to reduce the burden on the organelle (6). In order to execute these functions of the UPR, the ER needs to have proteins capable of detecting stress. The three main ER stress sensors are Activating Transcription Factor-6 (ATF-6), Protein Kinase RNA (PKR)-like ER Kinase (PERK),

and Inositol Requiring Enzyme-1 (IRE1) (7). For the purposes of this thesis, IRE1α will serve as the focal ER stress sensor.

1.3 IRE1α

IRE1 exists in two isoforms, IRE1α and IRE1β. IRE1α is present in virtually all tissue types while IRE1β is restricted to express only in intestinal epithelial cells (8). This thesis will focus on the IRE1α isoform. IRE1α exists as a transmembrane protein, having an N-terminal domain within the ER lumen, a transmembrane domain, and a C-terminal cytosolic domain with kinase and endoribonuclease activity (9). The N-terminal domain is crucial for sensing ER stress through a buildup of misfolded proteins. This occurs when binding immunoglobulin protien (BiP), a key molecular chaperone, detaches from the IRE1 N-terminal domain and preferentially binds misfolded proteins (8). Without BiP association, the N-terminal domain of IRE1 will self-associate with other IRE1α N-terminal domains, leading to polymerization and subsequent autophosphorylation of the C-terminal cytoplasmic domain (8). Once the conformational change occurs, indicating a buildup of misfolded proteins, the endoribonuclease domain will splice X-Box Binding Protein-1 (XBP-1) mRNA, creating XBP-1s (10). XBP-1s is the active form of the transcription factor that can proceed to enter the nucleus and upregulate the transcription of molecular chaperones and other proteins to promote proper protein folding (10). Furthermore, the endoribonuclease domain can also direct Regulated IRE1-Dependent Decay (RIDD) (11). RIDD functions to degrade specific mRNAs in an attempt to lessen the protein processing load of the cell. IRE1α is a complex protein and often exhibits context dependent effects, particularly in various forms of pathogenesis.

1.4 Role of IRE1α in Disease Pathogenesis

While IRE1α plays a vital role in maintaining normal physiological functions, it has been implicated in a variety of diseases such as Alzheimer's, cardiovascular disease, and cancer (12-15). In Alzheimer's disease, protein aggregates form to progressively impede neurological function resulting in neurodegeneration. It may stand to reason that upregulating the UPR through IRE1α activation may mitigate the deleterious buildup of protein aggregates, however that does not appear to be the case. Interestingly, researchers have observed a counterintuitive result that increased IRE1α activation corresponds to a higher degree of Alzheimer's disease pathology, measured by the amount of protein aggregates in the brains of Alzheimer's patients (12). Furthermore, the researchers found that genetic deletion of IRE1α in a mouse model, specifically of the endoribonuclease domain, significantly reduced beta-amyloid protein aggregates (12).

IRE1α has also been shown to play a crucial role in the development and progression of cardiovascular disease. Cardiovascular diseases are among the leading public health threats faced today. IRE1α activation due to ER stress plays a key role in cardiovascular disease such as atherosclerosis (13). During the development of atherosclerosis, lipid plaques deposit on the walls of blood vessels and induce a dangerous inflammatory state. The inflammatory state is in part driven through IRE1 mediated production of key proinflammatory cytokines. Researchers found that when they targeted IRE1α through small-molecular inhibitors, they were able to reduce plaque size and levels of hyperlipidemia-associated cytokines in atherosclerotic mice (14). Although it may seem that IRE1α and ER stress only perpetuate diseased states, this is not always the case. In patients with lung adenocarcinoma, higher levels of IRE1α actually predicted

lower disease stage, less invasion, and higher recurrence-free survival (15). There is no clear answer whether or not expression is harmful or beneficial in the development and maintenance of disease, and it appears to be highly context dependent. This thesis will help characterize the role of IRE1 in the response to another concerning and dangerous public health threat, Ultraviolet-B radiation (UVB).

1.5 UVB

Ultraviolet (UV) radiation is the major cause of the most common type of cancer worldwide, skin cancer (16). UV radiation can be further classified based on its wavelength, with each classification effecting the skin in different capacities. UVA (320-400nm) causes oxidative effects, UVB (290-320nm) is regarded as the most important because it is implicated as the cause of most UV radiation responses, and finally UVC (200-290nm) rarely ever reaches earth's surface, so it is of little concern (17). This thesis utilizes UVB during experimentation, so it will be the focus in this introduction.

Although often taken for granted, the skin is the largest and arguably one of the most important organs in the body. It serves key functions in defense and homeostasis. Disruptions to the skin can come from any number of environmental factors, but UVB remains the primary threat. UV radiation is classified as a "complete carcinogen" because it acts as a mutagen and a non-specific damaging agent (18). It also has been shown to act as both a tumor initiator and a tumor promoter (18). UVB induces a multitude of cellular responses within the resident cells of the skin, including apoptosis, DNA damage, ER stress, and cytokine release (18-24).

Apoptosis induced by UVB occurs through a few different routes. When UVB radiation reaches the epidermis and penetrates keratinocytes, it causes rapid free radical production resulting in an immediate type apoptosis (18). Researchers have also shown the Fas ligand (FasL) to play an important role in UV induced apoptosis (19). Finally, UVB also induces a more traditional type of apoptosis, caused by DNA damage (18).

DNA damage comes in a multitude of different forms such as DNA lesions, and strand breaks. With different damage induction methods, comes different biological systems to deal with said damage. While some DNA damage results in apoptosis, other damage engages systems like base excision repair (BER), and mismatch repair (MMR) (20). By engaging these systems, the cell attempts to control the damage and promote cell survival to a normal state. However, in the case of UVB exposure, a particular type of DNA lesion called a cyclobutene pyrimidine dimer (CPD) predominates (21). A CPD will form between neighboring pyrimidine bases upon irradiation with UVB. They can be particularly damaging because it has been experimentally shown that induction of CPDs can activate mutations in a crucial tumor suppressor gene, tumor protein 53 (P53) (21). In one study, researchers found that P53 mutations were found in 58% of invasive squamous cell carcinomas, one of the three primary forms of skin cancer (22). This suggest UVB induced CPD forming DNA damage could represent a pathway leading to skin carcinogenesis. In short, UVB represents a dangerous environmental stimulus that perturbs normal physiological homeostasis. As such, UVB has also been shown to induce the ER stress response (23).

Considering the ER stress pathway, and IRE1α in particular is a focal point of this thesis. It is important to inform about current knowledge of the relationship between UVB and ER stress. Relatively recently, researchers provided evidence that UVB radiation is capable of inducing the

ER stress response UPR pathway (23). Particularly interesting is the finding that XBP-1 expression, the transcription factor regulated by IRE1 activity, was upregulated upon UVB exposure (23). Other arms of the UPR were either downregulated or unaltered suggesting a crucial role for IRE1α within the context of UVB induced ER stress.

Another ER-related cellular process altered by UVB exposure is cytokine production (24). Cytokines are the primary cell signaling molecules of the body. They have countless different functions and allow for communication between cells near and far. They often have complex and context dependent effects. Under UVB exposure however, it appears that cytokine production is altered in a manner that gives rise to an inflammatory state (24).

1.6 Inflammation

Inflammation in a simple sense is the body's response to harmful stimuli. Stimuli can be any number of environmental or internal factors that the body recognizes as harmful. If the stimulus is transient, the inflammatory response is termed an acute response. If the stimulus persists, a state of chronic inflammation ensues. Inflammation has been linked to the development of skin cancer thus it is crucial to understand the initiation and maintenance mechanisms of inflammation (25). In this case, UVB is a principal example of a harmful stimuli that induces an inflammatory state through cytokine and chemokines signaling from keratinocytes. Two cytokines, shown to be induced by UVB radiation, are the pro-inflammatory cytokines Interleukin-6 (IL-6) and Tumor Necrosis Factor-α (TNFα) (26).

IL-6

Interleukin-6 is a soluble inflammatory mediator with diverse functions within organisms. IL-6 was originally termed B-Cell Stimulating Factor-2 (BSF-2) due to its ability to induce immunoglobulin production upon bacterial or viral stimulation (27). However, BSF-2 was subsequently found to be the same protein as hepatocyte-stimulating factor, Interferon-β2, and the hybridoma growth factor so it was renamed IL-6. The cytokine is capable of inducing B-cell differentiation, cytotoxic T-cell differentiation, acute phase protein production, platelet production, and nerve cell differentiation (28). Given these functions, IL-6 has long been considered a hallmark cytokine of an inflammatory response. IL-6's expression will be analyzed in this thesis, in response to UVB.

TNFα

Another key cytokine in an inflammatory response is Tumor Necrosis Factor-α or TNFα. TNFα, like IL-6, is a multifunctional cytokine that has been studied for decades to understand the innumerous roles in normal physiology, and various diseases. In humans, he cytokine is synthesized as a 27-kDa monomer that undergoes cleavage to yield the 17-kDa soluble signaling molecule (29). Upon binding to the TNFα receptor-1 (TNFR1), TNFα transduces a signal to two cascades, mitogen-activated protein kinase (MAPK) and nuclear factor kappa-light-chain-enhancer of activated B-cells (NFκB) (29). These signals are translocated to the nucleus where they upregulate genes associated with anti-apoptosis, proliferation, and inflammation. TNFα's expression will also be analyzed in this thesis in a similar manner to IL-6's. The TNFα and IL-6 induced inflammatory state is characterized by an infiltration of leukocytes, which can be identified by a transmembrane glycoprotein called common leukocyte antigen, or CD45 (30).

CD45

CD45 is a receptor-linked protein phosphatase that is expressed on the nucleated cells of hematopoietic origin (31). Although CD45 is expressed ubiquitously on leukocytes, the protein plays a key role in lymphocytes. In T-cells, CD45 expression is required for activation via the T-cell receptor (TCR) (32). Additionally, B-cells deficient in CD45 were shown to be unable to properly activate downstream signaling cascades (33). For the purposes of this thesis, CD45 will only serve as a marker for leukocytes within the skin.

Ki67

As previously mentioned, inflammation and the down-stream signal transduction can induce cellular proliferation. To investigate IRE1α-controlled, UVB induced cellular proliferation in this thesis, we used the nuclear marker Ki67. Ki67 is conveniently expressed only during all active stages of the cell cycle (G1, S, G2, and mitosis), yet it is not expressed during the resting phase (G_0)(34). This makes the protein ideal for looking at proliferation in response to various stimuli. Because of how reliably Ki67 levels reflect cell proliferation, it is often used as a prognostic marker in clinical pathology related to various cancers where greater levels of Ki67 correlate with a less favorable prognosis (34). Particularly in skin cancer, it has been shown that squamous cell carcinomas, primarily caused by UVB, show high levels of Ki67 positive cells (35).

1.7 Angiogenesis

Although inflammation and cell proliferation are part of the body's response to UVB, they are certainly not the only response. Another key physiological process that can be induced by UVB and other stimuli is Angiogenesis. Angiogenesis is another normal physiological process that can become dysregulated with environmental stimuli or through disease development. Angiogenesis is the creation of new blood vessels, sometimes referred to as neovascularization. The process is important for proper growth and development of organisms however it can contribute to diseases such as cancer, various forms of blindness, and arthritis (36). As angiogenesis is such an important process, it requires tight regulation by both pro-angiogenic and anti-angiogenic factors. Exposure to UVB in keratinocytes has been shown to induce production of a highly potent pro-angiogenic factor, vascular endothelial growth factor-A (VEGF-A) (37).

VEGF

The VEGF family of secreted proteins is an evolutionarily conserved set of four VEGF subtypes VEGF-A, VEGF-B, VEGF-C, and VEGF-D (37). For the purposes of this thesis, VEGF-A will be the focus, as it is most relevant and usually the most prominent in both normal physiology and diseases (38). VEGF-A was originally discovered as a signal for increasing vascular permeability but was subsequently shown to be a stimulator of angiogenesis (38). The presence of potent pro-angiogenic factors like VEGF-A necessitates a counterbalance of anti-angiogenic factors to keep the process in check.

SPARC

One anti-angiogenic factor that will be investigated in this thesis is secreted protein acidic and rich in cysteine (SPARC). SPARC is a glycoprotein with diverse, and often tissue specific functionality (39). Overall however, SPARC is well characterized for the ability to inhibit the activity of pro-angiogenic factors, such as VEGF (40). Additionally, the protein has been shown to enhance cellular proliferation (40). SPARC has been shown to exhibit variable effects on the development and progression of different forms of cancer development, depending on the context (40). In melanoma for instance, high SPARC expression correlated with increased invasiveness and poor prognosis (41). However, SPARC has also been shown to inhibit the progression of neuroblastoma (40). Even though the correlative relationship of SPARC to different cancers varies, it is classically regarded as anti-angiogenic based on it molecular mechanism.

1.8 Aim of Paper

This thesis aims to understand how IRE1α mediates the stress response to acute and chronic UVB exposure by altering gene expression and subsequent inflammation. To date, there is still a lack of understanding in how IRE1α and ER stress play a role in the response to UVB. Using an in-vivo, epidermally targeted IRE1α genetic ablation, we are able to examine the functionalities of the protein in keratinocyte signaling. This research can guide future mechanistic investigation of how IRE1 exhibits these effects. This research can also hopefully be used in the future to guide therapeutic strategies to negate the carcinogenic or otherwise dangerous effects of UVB exposure.

Chapter 2

Materials and Methods

2.1 K14Cre IRE1α Flox/Flox model

In order to study the effects of IRE1α in keratinocyte signaling, upon UVB irradiation, our lab uses a transgenic mouse model that selectively ablates IRE1α expression in the epidermis. The transgenic IRE1α Flox/Flox models features loxP sites flanking crucial exon 2 of IRE1α. The transgenic K14Cre mouse model features Cre recombinase protein, driven by the keratin 14 promoter, selectively expressed in the epidermis. When these two genotypes are successfully crossed, the resultant K14Cre x IRE1α Flox/Flox (IRE1α -/-) has Cre recombinase expression in the epidermis that induces intramolecular recombination of the DNA between loxP sites flanking exon 2. This creates a functional null IRE1α within the epidermis, allowing our lab to study how IRE1α signaling in keratinocytes effects different forms of pathogenesis, in this case UVB exposure. IRE1α Flox/Flox genotype by itself will serve as the wild type (IRE1α +/+) control.

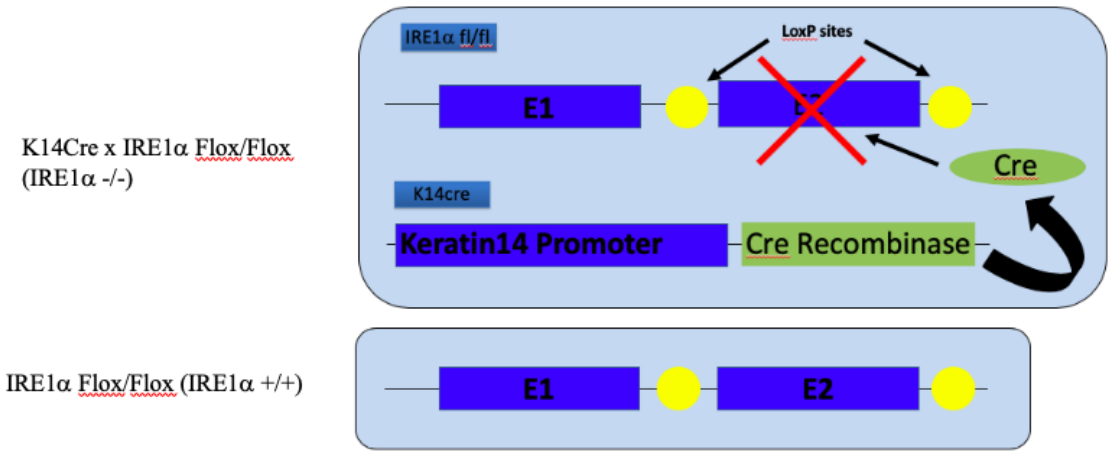

Figure 2: Conditional deletion of IRE1α in epidermal keratinocytes

2.2 DNA isolation and PCR Genotyping of mice

Polymerase-chain reaction (PCR) was used to determine the genotypes of potential experimental mice. IRE1α Flox/Flox mice are bred in a homozygous manner, so all offspring will necessarily have the IRE1α Flox/Flox genotype. However, K14Cre offspring must be genotyped to determine whether or not they have the K14Cre transgene. DNA isolation is carried out by taking a 0.25 inch tail snip from mice of interest at 21 days old. The small tail snip is then lysed with a buffer made from 100mM Tris-HCL pH 8, 5mM EDTA, 0.2% SDS, and 200mM NaCl in combination with Proteinase-K. The tail snip, along with 50 uL lysis buffer and 10 uL proteinase-K is placed in a thermomixer for 1 hour and 30 minutes at 61°C and 1300 rpm. The proteinase-k is then inactivated with a 5-minute incubation at 99°C. 400 ul of Low TE is then added to each sample and the sample is centrifuged for 2 minutes at 14000 rpm. Once DNA isolation is complete, PCR genotyping is done. DNA, K14Cre primers, and a PCR mastermix are combined, and amplified. The amplified DNA is then electrophoresed on an agarose gel and visualized under UV light. When a positive result is seen, as indicated by a strong single band, the mouse corresponding to the sample is determined to be K14Cre x IRE1α Flox/Flox and therefore have a functional null IRE1α (IRE1α -/-) within the epidermis. Mice that did not amplify K14Cre were only IRE1α Flox/Flox and served as wild-type (IRE1α +/+) control for the experiments.

2.3 UVB exposure

To induce UVB mediated inflammation, mouse backs were shaved and exposed to a 302 nm wavelength UV light at 240 mJ/cm2. The exposure was done to 8 week old males and females from IRE1α +/+ and IRE1α -/- groups. UVB exposure done during the experiments was delivered either acutely or chronically. Acute UVB exposure mice had a one-time exposure to UVB and were harvested at 24, 48, and 72 hours afterwards. Chronic UVB exposure mice had a total of 12 UVB exposures over the course of 6 weeks (2x exposure/week) and were harvested 24 hours following their last exposure.

2.4 Protein isolation and western blot analysis

Epidermal keratinocyte protein lysates were obtained using RIPA lysis buffer (50mM Tris-HCl pH 7.6, 150mM NaCl, 1% NP-40, 0.5% Sodium deoxycholate, 0.1% SDS, 1mM EDTA, 2mM Beta-glycerophosphate, 5mM NaF, 1mM PMSF, 1ug/ml Aprotinin, 5ug/ml Leupeptin, 1ug/ml Pepstatin, 2mM Sodium Orthovanadate). Epidermal scraping was combined with RIPA buffer and left rotating at 4°C for 1 hour. Next, the mixture was centrifuged at 14000 rpm for 15 minutes, and the supernatant was transferred to a new centrifuge tube.

To determine protein concentrations of each sample, a Pierce BCA protein assay (Thermo Fisher). A set of standards were prepared using BSA (2mg/ml) of concentrations 500μg/ml, 250 μg/ml, 150 μg/ml, 100 μg/ml, 50 μg/ml, and a blank sample. 2 μL of experimental samples were added, in duplicate, to a 96 well BD falcon plate, and had 48 μL of dye prepared from kit reagents added. The plate was allowed to incubate at 37°C for 30 minutes and then read in a Promega Glomax Multi-Detection plate reader at 570 nm wavelength.

To conduct the western blot, 20 μg protein samples were brought to equal volume using Laemmli protein loading dye and Nano-pure water. Samples were heated at 100°C for 10 minutes and then loaded into a 10% SDS-PAGE gel, along with a molecular ladder, and ran to completion at 100V. Upon completion, gels were transferred onto a nitrocellulose membrane using a Bio-Rad trans-blot TURBO transfer system. Separate strips of the membrane were cut to allow concurrent analysis of proteins of interest. Next, the membrane strips were incubated in a 5% blocking solution (5g blotto in 100mL TBS-Tween) for 1 hour at room temperature. The membrane strips were then washed with TBS-Tween before being incubated in 1:1000 dilutions of their respective anti-mouse primary antibody solutions overnight at 4°C. After the overnight primary antibody incubation, membrane strips were again washed with TBS-Tween before incubating in 1:1000 dilutions of respective secondary antibodies for 1 hour at room temperature. Finally, to develop, strips were washed with TBS-Tween and then had either ECL (Pierce) or Dura (Pierce) added for chemiluminescence visualization. Multiple exposure pictures were taken in succession using KwikQuant software. Primary antibodies for the blot included β-actin (Cell Signaling #3700), XBP-1s (Cell Signaling #12782), and IRE1α (Cell Signaling #3294).

2.5 RNA isolation, cDNA synthesis, and RT-qPCR

Keratinocyte RNA was isolated by first, collecting an epidermal scraping during mouse harvest. Then, RNA was extracted from keratinocytes using the Qiagen RNeasy® Mini Kit (#74104). After RNA extraction, a cDNA library was synthesized using master mix composed of M-MLV RT enzyme (Promega # M1705, 50,000U), 5X RT buffer (Promega# M5313), Random Primers (Promega# C1181, 20ug), and dNTPs(Denville Scientific # CB4421-4, 100mM). To

achieve a 100 ng/uL concentration, 2.5 ug total RNA was used per 25 uL reaction. 12.5 ul of master mix was combined with 12.5 ul of RNA + water, yielding 25 uL total. The samples were added to a thermocycler and ran for 10 minutes at 25°C, then 2 hours at 42°C, and finally 5 minutes, at 85°C. The cDNA product was then stored at -20°C until it was needed.

Once it was time to run real-time quantitative PCR (RT-qPCR), the cDNA was diluted by adding 2 uL of cDNA to 98 uL of water. 5 uL of each sample was added in duplicate to the corresponding wells of a standard 96 well PCR plate (Denville Scientific #1158U13), along with a 5-fold dilution series of random undiluted cDNA that would later be used as to generate a standard curve. 15 uL of RT-qPCR master mix was then added to each well, bringing each reaction volume to 20 uL. To normalize levels of mRNA, ß-actin served as a reference gene. Reactions were then ran using a MyiQ iCycler (BioRad). Primers for genes analyzed using qPCR are listed below.

Gene	Forward Sequence (5'-3')	Reverse Sequence (5'-3')
ß-actin	ACCAACTGGGACGATATGGAGAAGA	TACGACCAGAGGCATACAGGGACAA
TNFα	GATTATGGCTCAGGGTCCAA	GAGACAGAGGCAACCTGACC
IL-6	AACCGCTATGAAGTTCCTCTCTGC	TAAGCCTCCGACTTGTGAAGTGGT
VEGF	CTACCAGCGCATCCTCTCTC	GAGCCTTTAACAGGTGGGCT
SPARC	TGCCCAGAGCTCCAAGAGGCT	TCCCGGCCAGGCAAAGGAGAA

Figure 3: qPCR primers for selected genes

2.6 Immunohistochemistry and Immunofluorescence

Back skin tissue from UVB exposed area was collected during necropsy and either frozen in Tissue-Tek® O.C.T. Compound (Sakura) or fixed in formaldehyde and paraffinized at Penn State Huck Institute of the Life Sciences Microscopy Core Facility. Paraffinized samples were sectioned and placed on standard glass microscope slides for use in immunohistochemical staining.

Immunohistochemical staining for CD45, found on all leukocytes, began with deparaffinization and rehydration. Tissues were deparaffinized and rehydrated by incubating the tissues in Xylene (3x), 100% ethanol (1x), 90% ethanol (1x), 70% ethanol (1x), and 1XPhosphate Buffered Saline (PBS) (2x) for 5 minutes per incubation. In order to properly stain the tissues, we then used a heated citrate antigen retrieval buffer (10mM sodium citrate, 0.05% Tween 20 in ddH2O, pH 6). After antigen retrieval, tissues were washed in 1XPBS for 5 minutes. To quench endogenous peroxidase activity, tissues were incubated for 15 minutes in a 3% H_2O_2 solution. Samples were again washed in PBS for 5 minutes. Then, tissue samples were blocked to avoid non-specific antibody binding using a 10% Normal Goat Serum (Vector #1000) diluted in 3% Bovine Serum Albumin (BSA)(Fisher Scientific #BP1600-100/PBS at room temperature for 20 minutes. Samples were then incubated overnight at 4°C with a 1:250 dilution of purified rat anti-mouse CD45 (BDbiosciences #550539). Samples were washed the next morning for 5 minutes in PBS and then incubated with 1:500 dilution of biotinylated goat anti-rat IgG (Vector #BA-9401) at room temperature for 30 minutes. Samples were then washed twice for 5 minutes in PBS and then incubated for 30 minutes at room temperature with Strep-HRP.

Samples were washed twice for 5 minutes each in PBS. ImmPACT™ DAB (Vector #SK-4105) solution was prepared and placed on the tissue for 2 minutes and 30 seconds in the absence of direct light. Samples were placed directly into water to halt the reaction, then counterstained with Hematoxylin QS (Vector #H-3404) for 5 minutes. Finally, samples were rinsed in tap water for 3 minutes and then dehydrated by incubating 5 minutes each in 70% ethanol (1x), 90% ethanol (1x), 100% ethanol (1x), and then Xylene (3x). Slides were then cover slipped with HistoChoice® Mounting-Media (Amresco #H157-120ML). Tissues were visualized on an Olympus SC100 microscope at 200X magnification from 3 random fields. CD45+ cells were counted and averaged for IRE1α +/+ and IRE1α -/- groups.

For quantitative Ki67 immunohistochemistry, the same Immunohistochemical procedure was used with the exception of primary antibody incubation, secondary antibody, and quantitation. The rabbit anti-mouse Ki67 primary antibody (Cell Signaling Technologies #9129) was used in a 1:500 dilution. The secondary antibody used was a 1:250 dilution of biotinylated goat anti-rabbit IgG (Vector Labs #BA-1000). Finally, 5 fields were taken on an Olympus SC100 microscope at 200X magnification and Ki67 positive cells of the epidermis were quantified using QuPath version 0.1.2.

For qualitative Ki67 immunofluorescence, frozen tissue samples were sectioned using a cryostat microtome, then stored at -80°C until staining. When sectioned tissues were ready to be stained, they were first thawed at room temperature for 3 minutes, then rehydrated in cold PBS twice for 5 minutes each incubation. The tissues were then fixed with a 10 minute acetone incubation, using about 500 uL acetone per slide. To remove acetone fixative agent, 2 more 5 minute PBS incubations were done. To block non-specific anti-body binding, the same 10% normal goat serum blocking dilution used in IHC was prepared and incubated on the samples,

again for 20 minutes at room temperature. Following the blocking step, samples were incubated with 1:500 diluted rabbit anti-mouse Ki67 primary antibody (Cell Signaling Technologies #9129) overnight at 4°C. The samples were washed the next morning in PBS for 5 minutes. After washing off the primary anti-body, the samples were incubated using a 1:500 dilution of biotinylated goat anti-rabbit IgG (Vector #BA-1000) for 30 minutes at room temperature. The secondary was washed using another 2 incubations in PBS for 5 minutes each. All of the following steps were done in the absence of direct light. A 1:500 dilution of Streptavidin conjugated Alexa Fluor® 488 (JacksonImmunoResearch #016-540-084) was put on the samples for 30 minutes at room temperature. Following that, two more 5 minute PBS incubations were done to remove unbound fluorescent conjugate. Samples were then stained using one drop of mounting medium with Propidium Iodide (Vectashield #H-1300) and cover slipped. Samples were examined under a Olympus CKX41 microscope and fluorescent images were taken using an Olympus XC10 camera at 200X magnification. 500 ms exposure was used for Alexa Fluor® 488 visualization (green/Ki67) while 150 ms exposure was used for propidium iodine (red/all nucleated cells).

Chapter 3

Results

3.1 IRE1α Knockout was successful, and UVB alters IRE1α protein expression and activation

To determine if there was successful IRE1α knockout, and if UVB induces the ER stress response in our mouse models, protein harvested from the acute UVB exposure group was analyzed for expression of IRE1α, spliced XBP-1, and ß-actin. Protein was isolated at 24, 48, and 72 hours after acute UVB exposure. Figure 3 indicates that UVB induces IRE1α upregulation as well as downstream XBP-1 splicing in the IRE1α Flox/Flox mice (IRE1α +/+), indicating UPR activation. Figure 3 also shows that K14Cre x IRE1α Flox/Flox (IRE1α -/-) mice had no meaningful IRE1α or XBP-1 expression basally or following UVB treatment, indicating that genetic ablation of IRE1α in the epidermis was successful. Slight double bands can be seen in IRE1α -/- likely representing the truncated inactivated form of the protein caused by the congenital splicing. There is also slight XBP-1s in the IRE1α -/- group, potentially from IRE1α independent mechanisms

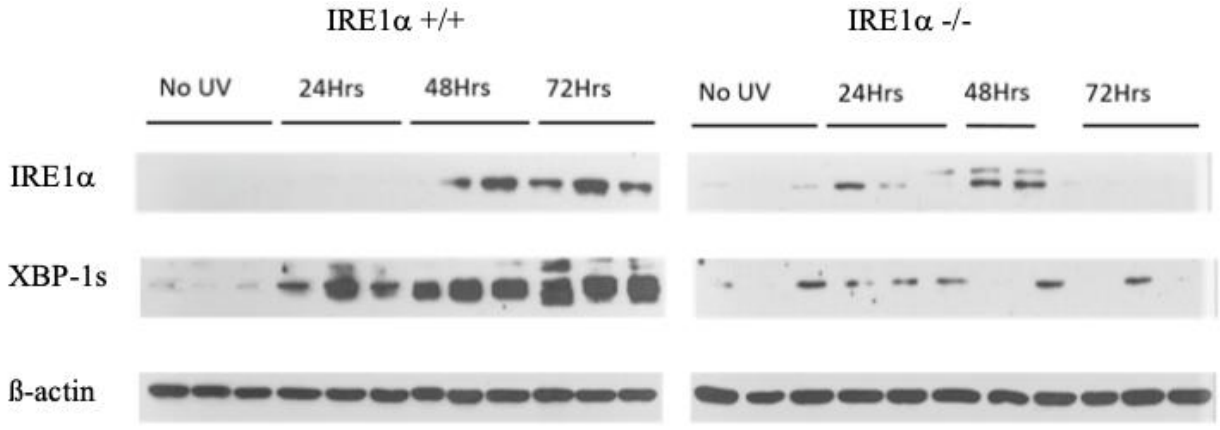

Figure 4: Western blot analysis of IRE1α, XBP1-s, and actin in WT and KO epidermal keratinocytes at 0, 24, 48, and 72 hours after UVB exposure.

3.2 Epidermal IRE1α deletion alters proinflammatory cytokine expression in response to acute UVB exposure

Once we confirmed that epidermal IRE1α knockout was successful, we next wanted to test whether or not expression of proinflammatory genes was altered by the presence of IRE1α following a single exposure of UVB. To test this, IRE1α +/+ mice and IRE1α -/- mice were exposed to UVB and harvest at 48, and 72 hours post exposure. In addition, non-exposed mice from each group were also harvested. The epidermal keratinocytes were isolated, and RTq-PCR was done to determine gene expression. IL-6 and TNFα were the proinflammatory genes of interest. Figure 5 shows that without IRE1α, epidermal keratinocytes exhibited significantly suppressed levels of IL-6 expression and decreased levels of TNFα expression following a single UVB exposure, suggesting a proinflammatory role of IRE1α after acute UVB exposure.

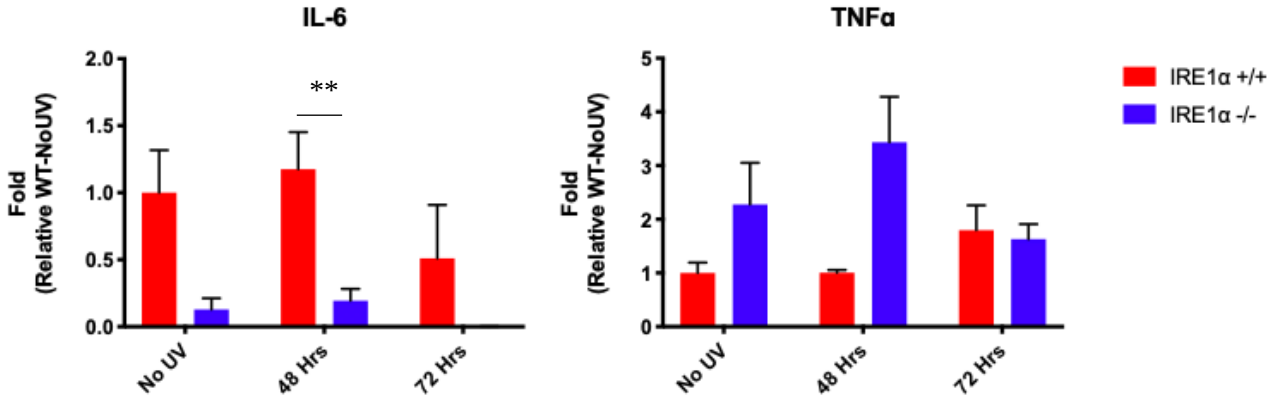

Figure 5: IRE1α deletion alters expression of proinflammatory IL-6 and TNFα genes after acute UVB exposure

3.3 Epidermal IRE1α deletion reduces leukocyte infiltration in response to acute UVB exposure

After observing that IRE1α deletion can control proinflammatory cytokine gene expression, we wanted to determine if deletion of IRE1α also controls leukocyte infiltration into the skin following acute UVB. To test this, we exposed IRE1α +/+ and IRE1α -/- mice to UVB and harvested groups of 3 with no-exposure and at 24, 48, and 72 hours after exposure and conducted CD45 immunohistochemistry on mouse skin sections. Results show that IRE1α deletion reduced overall leukocyte infiltration, measured by CD45+ cells. Reduced leukocyte infiltration in IRE1α appears to continue at all time points after UVB exposure. Figure A shows pictures representative of the observed pattern, while figure B is the quantitation.

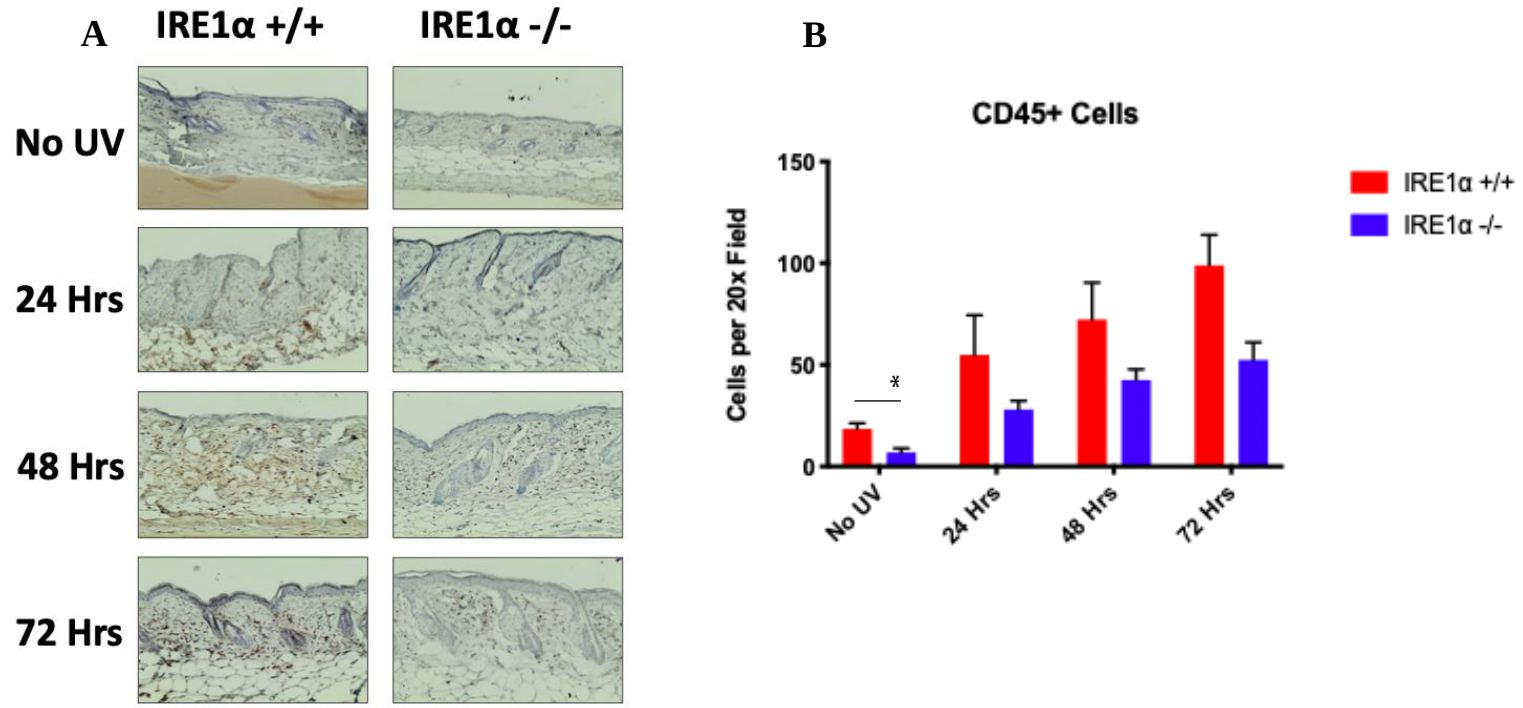

Figure 6: Epidermal IRE1alpha deletion reduces inflammatory leukocyte infiltration. (A) Representative images of CD45 immunohistochemical staining of IRE1alpha +/+ and IRE1alpha -/- mouse skin with no UVB exposure, and at 24, 48, and 72 hours after UVB exposure. (B) Quantitation of CD45+ cells within 20x field of each group.

3.4 IRE1α mediates angiogenic gene expression in response to acute UVB exposure

As mentioned in the introduction, an important response to UVB exposure is angiogenesis, or the creation of new blood vessels. During this investigation, we wanted to see if IRE1α controls this process. To do so, we tested the expression of proangiogenic VEGF and anti-angiogenic SPARC after an acute UVB exposure in IRE1α +/+ and IRE1α -/- mice. Results show that an epidermal IRE1α deletion caused a significant decrease in VEGF expression and a significant increase in SPARC expression in mouse skin at 72 hours after UVB exposure. This indicates that IRE1α contributes to increasing the pro-angiogenic response and suppressing the anti-angiogenic response after acute UVB exposure.

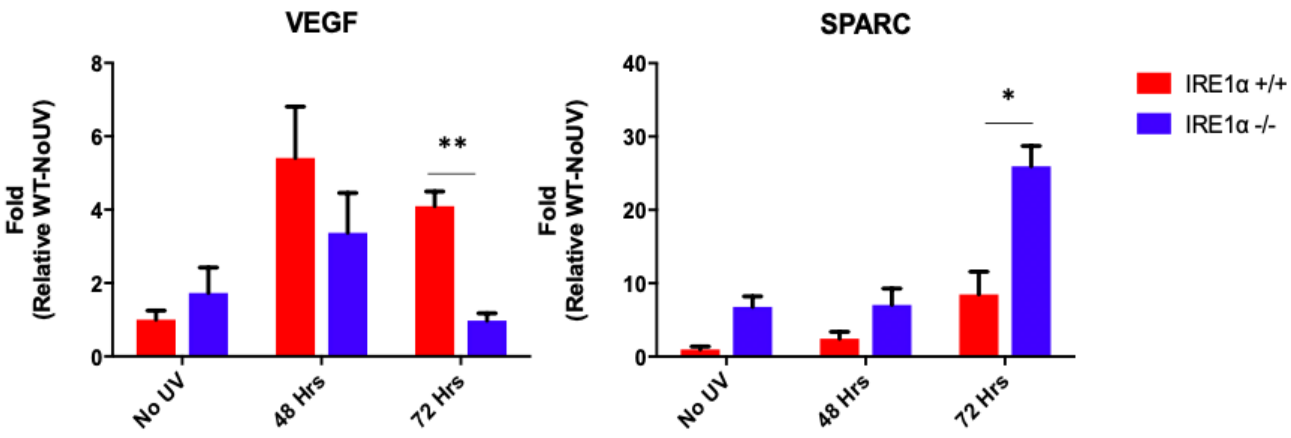

Figure 7: Epidermal IRE1α deletion decreases pro-angiogenic VEGF gene expression and increases anti-angiogenic SPARC gene expression in response to acute UVB exposure

3.5 Epidermal IRE1α deletion alters proinflammatory cytokine expression after chronic UVB exposure

After observing that IRE1α deletion in the epidermis altered proinflammatory cytokine expression following acute exposure, we wanted to investigate if the response differed following chronic exposure to UVB. To do so, we exposed IRE1α +/+ and IRE1α -/- mice to 12 treatments of UVB over the course of 6 weeks. Again, we used qRT-PCR to measure gene expression of proinflammatory cytokines IL-6 and TNF-α following the final exposure. In contrast with the acutely exposed groups, there were virtually no differences between IRE1α +/+ and IRE1α -/- groups in terms of IL-6 expression with both showing increased expression after chronic exposure to UVB. However, when examining TNFα expression, IRE1α +/+ mice had a significant reduction in expression of TNFα after chronic UVB exposure, suggesting an immunosuppressive effect of chronic treatment. In IRE1α -/- mice, this effect was opposite, and these mice showed some increase in epidermal keratinocyte TNFα expression after chronic UVB exposure. This indicates IRE1α could be involved in immunosuppression, in contrast to acute exposure where it was seen to promote inflammation.

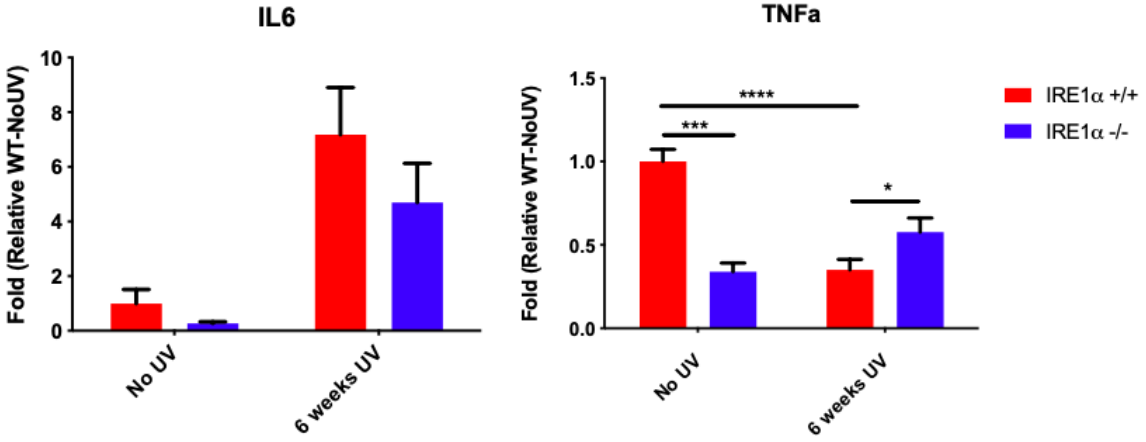

Figure 8: Epidermal IRE1α deletion alters pro-inflammatory gene expression of TNFα following chronic UVB exposure

3.6 Epidermal IRE1α deletion alters expression of angiogenic genes following UVB exposure

To further investigate IRE1α's control of angiogenic genes, we tested VEGF and SPARC in the chronic exposed IRE1α +/+ and IRE1α -/- groups before and after UVB. Like the results in the acute exposure groups, there was a significant increase in proangiogenic VEGF gene expression following chronic exposure. This increase was absent in IRE1α -/- mice that showed no change in VEGF expression before and after UVB exposure. Anti-angiogenic SPARC gene expression also followed a similar pattern to the acute exposure groups, where IRE1α -/- mice showed increased expression of SPRAC following chronic UVB exposure. These results suggest that IRE1α mediates a pro-angiogenic response to UVB in both acute and chronic exposures.

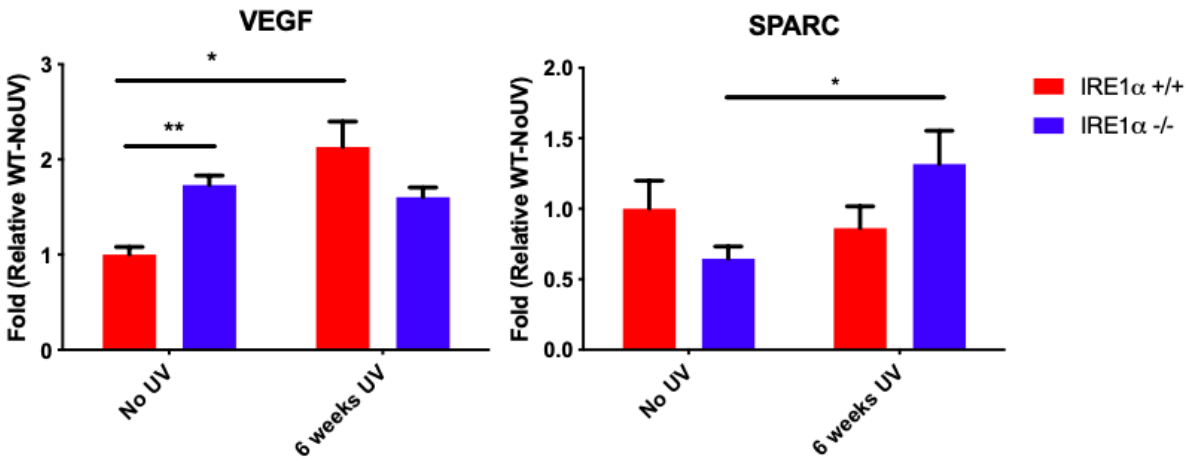

Figure 9: Following chronic UVB exposure, IRE1α +/+ mice showed significant increase in pro-angiogenic VEGF that was absent in IRE1α -/- mice. In contrast, IRE1 -/- mice showed a significant increase in anti-angiogenic SPARC after chronic UVB exposure that was absent in IRE1α +/+ mice.

3.7 IRE1α deletion suppresses basal, and chronic UVB induced cell proliferation

Cellular inflammation is an important response to UVB and if dysregulated can result in carcinogenic transformation. After observing that IRE1α controls the inflammatory and angiogenic responses after acute and chronic UVB exposure, we wanted to investigate if the ER stress sensor also controlled cell proliferation. To explore this, we examined Ki67 expression in the chronic exposure IRE1α +/+ and IRE1α -/- mice using Immunofluorescence and Immunohistochemistry. Ki67 is commonly used a molecular marker of cellular proliferation in basic science and as a prognostic cancer maker. First, Immunofluorescence was used to qualitatively examine Ki67 expression. Without UVB exposure, there is no visible Ki67 expression in the epidermis. However, there is some epidermal Ki67 expression after chronic UVB exposure, that appears greater in IRE1α +/+ mice.

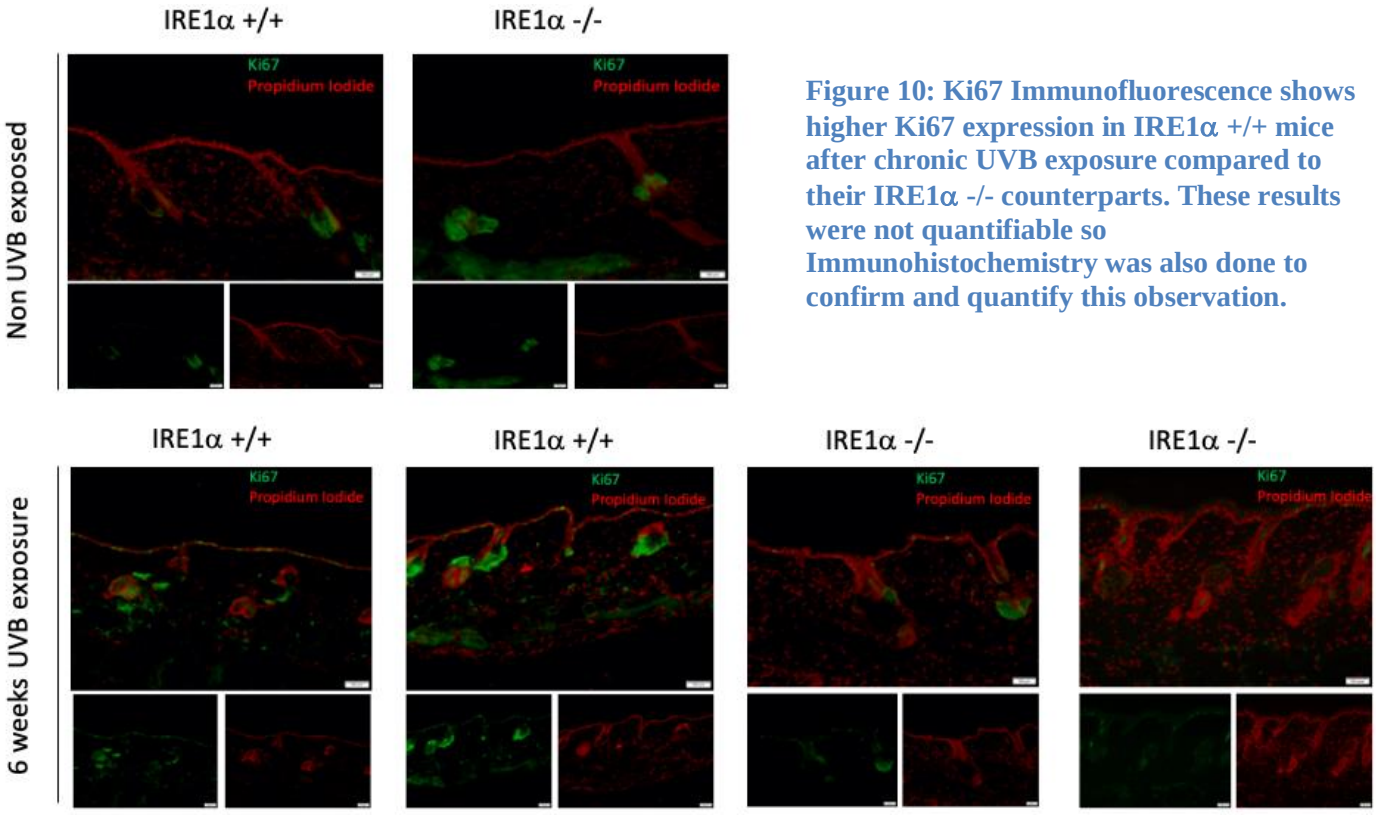

Figure 10: Ki67 Immunofluorescence shows higher Ki67 expression in IRE1α +/+ mice after chronic UVB exposure compared to their IRE1α -/- counterparts. These results were not quantifiable so Immunohistochemistry was also done to confirm and quantify this observation.

The results of the Ki67 immunofluorescence suggested that IRE1α deletion suppresses cell proliferation in response to UVB exposure. However, because immunofluorescence in this case was only qualitative, immunohistochemistry and the computer software QuPath were used to confirm and quantify this observation.

C

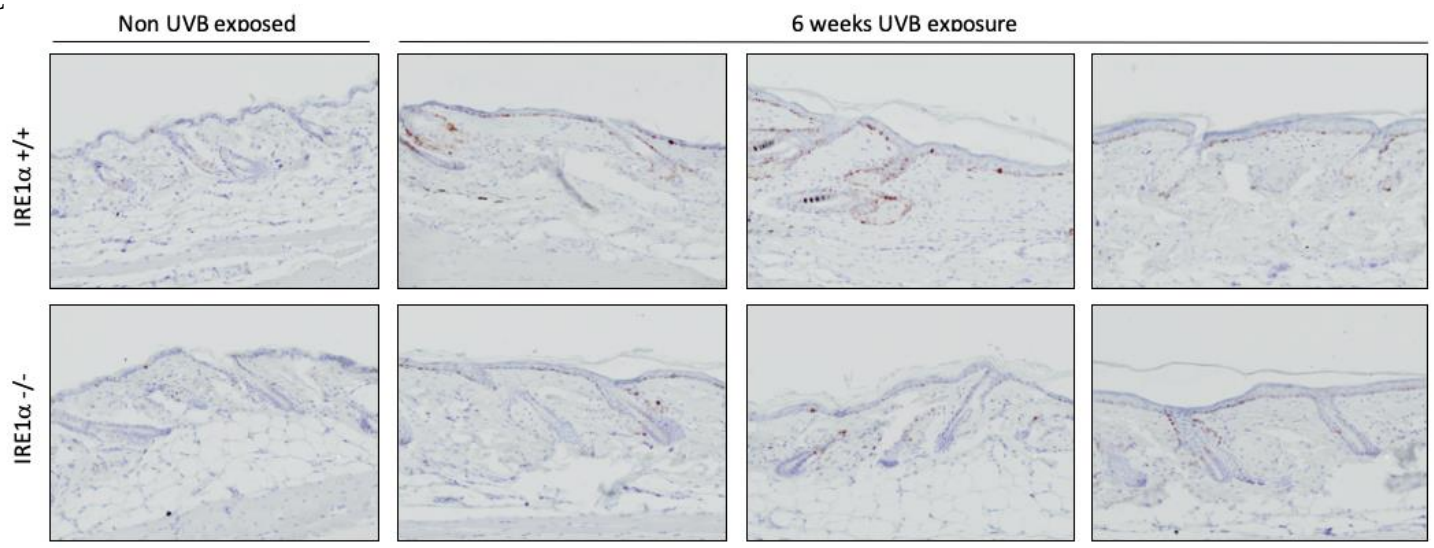

D

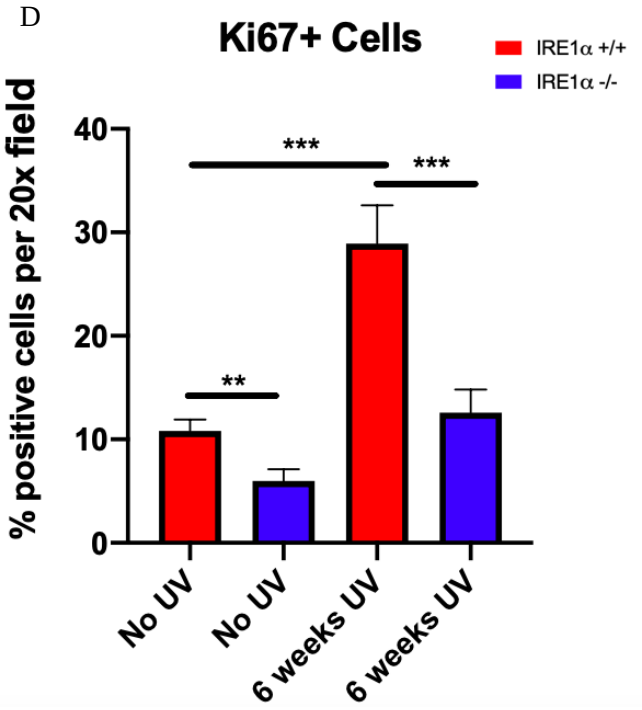

Figure 11: Epidermal IRE1α deletion reduces cell proliferation, as indicated by Ki67 (C) Immunohistochemistry for Ki67 shows that IRE1α +/+ mice have more Ki67+ cells without UVB exposure, and following 6 weeks of chronic UVB exposure (D) QuPath software was used to quantify Ki67+ cells as a percent of all epidermal cells. Results show that IRE1α +/+ mice had a significantly higher percentage of Ki67+ cells with no UVB. There was also a significant increase in percent Ki67+ cells in the IRE1α +/+ mice following chronic UVB exposure, whereas IRE1α -/- showed no significant increase.

Chapter 4 Discussion

4.1 Overview

The unfolded protein response (UPR) is a highly conserved mechanism whereby cells attempt to attenuate damage from misfolded or unfolded proteins induced by a number of different mechanism (5). These mechanisms often involve environmental insults, such as UV radiation, and the misfolded proteins that result contribute to various diseases, like cancer (15). To mitigate misfolded proteins, the UPR upregulates molecular chaperones, slows translation, and degrades mRNA (6). The stress caused by unfolded proteins is localized in the endoplasmic reticulum and it is termed ER stress. The three sensors of ER stress are ATF-6, PERK, and the focus of this thesis, IRE1α (7).

The primary goal of the research presented in this thesis is to characterize how the presence of IRE1α in epidermal cell affects cellular response to acute and chronic UVB exposure. UVB is the primary cause of skin cancer and represents a significant public health threat (16). It is also a known activator of ER stress, so IRE1α was presumed to play a role in UVB response (23). The specific cellular responses investigated were inflammation, angiogenesis, and cell proliferation, three hallmarks of cancer development. By using an epidermally targeted congenital deletion of IRE1α, we were able to see how the presence or absence of the protein affected these responses using different molecular techniques and immunoassays. Here, we showed that after an acute UVB exposure, epidermal IRE1α signaling contributes to alterations in inflammatory gene expression and an increase in inflammatory infiltrates. We also showed that after an acute exposure, epidermal IRE1α signaling is a key for

regulating the angiogenic axis, specifically upregulating pro-angiogenic VEGF and down regulating anti-angiogenic SPARC. In the more physiologically relevant, chronic UVB exposure group, epidermal IRE1α signaling was also shown to have profound impact. Similar to the acute exposure group, epidermal IRE1α signaling appears to promote angiogenesis in response to chronic UVB through up-regulating pro-angiogenic VEGF and downregulation of anti-angiogenic SPARC. However, in contrast to the acute UVB exposure group, IRE1α +/+ mice in the chronic UVB exposure group showed a decrease in proinflammatory TNFα expression, suggesting a potential immunosuppressive role for IRE1α following chronic UVB exposure. Additionally, we found that the presence of epidermal IRE1α correlated with a significant increase in cellular proliferation, as measured by Ki67.

The cellular processes induced by UVB, shown to be controlled by epidermal IRE1α in this thesis, are highly important in cancer development. Inflammation has previously shown to be directly linked to skin cancer development specifically (25). Angiogenesis is also commonly associated with cancer development, because tumors need blood supply to grow and proliferate. For the first time, we have shown IRE1α to be a key controller of angiogenesis induced by UVB, that could directly contribute to cancer development. The chief characteristic of cancer is excess cell proliferation, and skin cancer is no different. Here we have shown for the first time that epidermal IRE1α signaling is crucial for cell proliferation in response to carcinogenic chronic UVB.

In summary, this data suggests that epidermal IRE1α contributes to pro-angiogenic, and proliferative phenotype in mice after UVB exposure. This phenotype is classically indicative of cancerous transformation, which suggests research into the topic should be continued and

expanded upon. It is especially vital to expand this research because IRE1α and ER stress often exhibit context-dependent effects that are difficult to generalize. By understanding IRE1α's role in the response to UVB, this thesis could help create more effective therapeutics to combat highly prevalent, and potentially deadly skin cancers.

4.2 Future experiments

There are a few future experiments that could further elucidate the role of IRE1α in cancerous transformation. First, it is important to expand upon the results shown in this model of UVB exposure. In the future, other inflammatory and angiogenic genes should be investigated to better characterize IRE1α's role in regulating those responses. Particular genes of interest include pro-inflammatory genes IL-8 and IL-17 because of their notable roles in contributing to brisk inflammatory infiltration. Also the pro-angiogenic gene hypoxia inducible factor HIF-1-alpha because of its ability to promote cell survival and tumorigenesis along with anti-angiogenic genes decorin and thrombospondin-1 because of their ability to decrease the creation of new blood vessels. Finally, future experiments in this model of UVB exposure should include analysis of factors related to DNA damage apoptosis. Unpublished data in primary mouse keratinocytes has shown IRE1α to regulate expression of DNA damage marker H2A histone family member X (H2AX), which could help explain why IRE1α-/- mice have less cell proliferation in their epidermis. Another contributing factor could be a difference in apoptosis levels after UVB exposure. By analyzing the presence of pro-apoptotic factors, such as cleaved PARP, we could synthesize more clear picture of how IRE1α alters the cell response to stress.

Another important experiment is to investigate UVB-induced P53 mutations in our model. Differences in mutation levels of this key tumor suppressor could provide valuable insight into IRE1α control of carcinogenic transformation due to UV exposure.

It will also be important to elucidate the mechanisms of IRE1α's control over these various cytokines and factors. By attributing IRE1α's control over specific cytokines and factors to certain IRE1α effector functions, more specialized therapeutics could be created. For example, SPARC has been shown to be an RIDD target in a model of glioma (42). If this finding is confirmed in our model of UVB induced damage, we could modulate the IRE1α RIDD pathway specifically to alter SPARC expression to mitigate the inflammatory and carcinogenic processes. Alternatively, VEGF production has been shown to be controlled by XBP1, the main transcription factor regulated by IRE1α (43). If this mechanism is verified in our model, we could modulate VEGF expression through specifically targeting IRE1α splicing of XBP1. Beyond analyzing more processes in this model of IRE1α's regulation of carcinogenic UVB stress responses, it will be important to see if these results are similar across different models.

A vital future experiment is extending the UVB radiation in an attempt to induce tumors in IRE1α +/+ and IRE1α -/- mice. This is easier said than done because of the variability among UV-induced carcinogenesis models. Although time consuming, the experiment would be very valuable to test the observations seen in this thesis. We could measure the same genes and proteins to see if the differences we have seen correlate with any morphological differences after extended UVB exposure. If there are morphological differences between IRE1α +/+ and IRE1α -/- mice in terms of tumor numbers, tumor volumes, or survival, we could further contend that IRE1α plays a strong role in UV-induced cancer development.

Another model worth investigating these parameters in is a mouse model used by the Glick lab that induces Ras-driven lung cancer. It would be beneficial to investigate inflammation, angiogenic, and cell proliferation markers in this model to see if IRE1α deletion manifests similar changes in response to Ras-driven ER stress. This information might help to inform on whether or not IRE1α could be a useful therapeutic target in preventing or treating various conditions, or if IRE1α's effects of inflammation, angiogenesis, and cell proliferation are context-dependent.

BIBLIOGRAPHY

1. Schwarz, D.S. & Blower, M.D. 2016. The endoplasmic reticulum: structure, function and response to cellular signaling, *Cell Molecular Life Sciences*, 73: 79-94.

2. Braakman, I. & Hebert, D. N. 2013. Protein folding in the endoplasmic reticulum. *Cold Spring Harbor perspectives in biology*, *5*(5), a013201.

3. Ellis, R. J. & Van Der Vies, S. M. 1991. Molecular Chaperones. *Annual Review Biochemistry*, 60: 321-347.

4. Wang, S. & Kaufman, R. J. 2012. The impact of the unfolded protein response on human disease. *Journal Cell Biol*ogy, *197*(7), 857–867.

5. Schroder, M. & Kaufman, R. J. 2005. ER stress response and the unfolded protein response. *Mutation Research Fundamental and Molecular Mechanisms of Mutagenesis*, 569: 29-63.

6. Bravo, R., Parra, V., Gatica, D., Rodriguez, A. E., Torrealba, N., Paredes, F., Wang, Z. V., Zorzano, A., Hill, J. A., Jaimovich, E., Quest, A. F., & Lavandero, S. 2013. Endoplasmic reticulum and the unfolded protein response: dynamics and metabolic integration. *International review of cell and molecular biology*, *301*, 215–290

7. Gardner, B. M., Pincus, D., Gotthardt, K., Gallagher, C. M., & Walter, P. 2013. Endoplasmic reticulum stress sensing in the unfolded protein response. *Cold Spring Harbor perspectives in biology*, *5*(3), a013169.

8. Junjappa, R. P., Patil, P., Bhattarai, K. R., Kim, H. R., & Chae, H. J. 2018. IRE1α Implications in Endoplasmic Reticulum Stress-Mediated Development and Pathogenesis of Autoimmune Diseases. *Frontiers in immunology*, *9*, 1289.

9. Ali, M. M., Bagratuni, T., Davenport, E. L., Nowak, P. R., Silva-Santisteban, M. C., Hardcastle, A., McAndrews, C., Rowlands, M. G., Morgan, G. J., Aherne, W., Collins, I., Davies, F. E., & Pearl, L. H. 2011. Structure of the Ire1 autophosphorylation complex and implications for the unfolded protein response. *The EMBO journal*, *30*(5), 894–905.

10. Uemura, A., Oku, M., Mori, K., & Yoshida, H. 2009. Unconventional splicing of XBP1 mRNA occurs in the cytoplasm during the mammalian unfolded protein response. *Journal of Cell Science*, *122*(16), 2877–2886.

11. Maurel, M., Chevet, E., Tavernier, J., & Gerlo, S. (2014). Getting RIDD of RNA: IRE1 in cell fate regulation. *Trends in Biochemical Sciences*, *39*(5), 245–254.

12. Duran-Aniotz, C., Cornejo, V. H., Espinoza, S., Ardiles, Á. O., Medinas, D. B., Salazar, C., … Hetz, C. 2017. IRE1 signaling exacerbates Alzheimer's disease pathogenesis. *Acta Neuropathologica*, *134*(3), 489–506.

13. Minamino, T., Komuro, I., Kitakaze, M. 2010 Endoplasmic reticulum stress as a therapeutic target in cardiovascular disease. *Circulation Research,* 107(9): 1071-1082.

14. Tufanli, O. T., Akillilar, P. I., Acosta-Alvear, D. M., Kocaturk, B. undefined, Onat, U. undefined, Hamid, S. undefined, … Erbay, E. undefined. 2017. Targeting IRE1 with small molecules counteracts progression of atherosclerosis. *Proceedings of the National Academy of Sciences*, *114*(8).

15. Sakatani, T., Maemura, K., Hiyama, N., Amano, Y., Watanabe, K., Kage, H., Fukayama, M., Nakajima, J., Yatomi, Y., Nagase, T., & Takai, D. 2017. High expression of IRE1 in lung adenocarcinoma is associated with a lower rate of recurrence. *Japanese journal of clinical oncology*, *47*(6), 543–550.

16. Cancer Facts & Figures 2019. (n.d.). Retrieved from https://www.cancer.org/research/cancer-facts-statistics/all-cancer-facts-figures/cancer-facts-figures-2019.html

17. Sesto, A., Navarro, M., Burslem, F., & Jorcano, J. L. 2002. Analysis of the ultraviolet B response in primary human keratinocytes using oligonucleotide microarrays. *Proceedings of the National Academy of Sciences of the United States of America*, *99*(5), 2965–2970.

18. D'Orazio, J., Jarrett, S., Amaro-Ortiz, A., & Scott, T. 2013. UV radiation and the skin. *International journal of molecular sciences*, *14*(6), 12222–12248.

19. Leverkus, M., Yaar, M., & Gilchrest, B. A. 1997. Fas/Fas Ligand Interaction Contributes to UV-Induced Apoptosis in Human Keratinocytes. *Experimental Cell Research*, *232*(2), 255–262.

20. Rastogi, R. P., Richa, Kumar, A., Tyagi, M. B., & Sinha, R. P. 2010. Molecular mechanisms of ultraviolet radiation-induced DNA damage and repair. *Journal of nucleic acids, 2010,* 592980.

21. You, Y.-H. 2000. Cyclobutane pyrimidine dimers form preferentially at the major p53 mutational hotspot in UVB-induced mouse skin tumors. *Carcinogenesis*, *21*(11), 2113–2117.

22. Brash, D. E., Rudolph, J. A., Simon, J. A., Lin, A., McKenna, G. J., Baden, H. P., Halperin, A. J., & Pontén, J. 1991. A role for sunlight in skin cancer: UV-induced p53 mutations in squamous cell carcinoma. *Proceedings of the National Academy of Sciences of the United States of America*, *88*(22), 10124–10128.

23. Park, K., Lee, S. E., Shin, K. O., & Uchida, Y. 2019. Insights into the role of endoplasmic reticulum stress in skin function and associated diseases. *The FEBS journal*, *286*(2), 413–425.

24. Yoshizumi, M., Nakamura, T., Kato, M., Ishioka, T., Kozawa, K., Wakamatsu, K., & Kimura, H. 2008. Release of cytokines/chemokines and cell death in UVB-irradiated human keratinocytes, HaCaT. *Cell Biology International*, *32*(11), 1405–1411.

25. Maru, G. B., Gandhi, K., Ramchandani, A., & Kumar, G. 2014. The Role of Inflammation in Skin Cancer. *Advances in Experimental Medicine and Biology Inflammation and Cancer*, 437–469.

26. Lee, S. J., Lee, K. B., Son, Y. H., Shin, J., Lee, J. H., Kim, H. J., Hong, A. Y., Bae, H. W., Kwon, M. A., Lee, W. J., Kim, J. H., Lee, D. H., Jeong, E. M., & Kim, I. G. 2017. Transglutaminase 2 mediates UV-induced skin inflammation by enhancing inflammatory cytokine production. *Cell death & disease*, *8*(10), e3148.

27. Keller, E. T. 1996. Molecular and cellular biology of interleukin-6 and its receptor. *Frontiers in Bioscience*, *1*(4), d340–357.

28. Naka, T., Nishimoto, N., & Kishimoto, T. 2002. The paradigm of IL-6: from basic science to medicine. *Arthritis research*, *4* (Suppl 3), S233–S242.

29. Parameswaran, N., & Patial, S. 2010. Tumor necrosis factor-α signaling in macrophages. *Critical reviews in eukaryotic gene expression*, *20*(2), 87–103.

30. Clement, L. T. 1992. Isoforms of the CD45 common leukocyte antigen family: Markers for human T-cell differentiation. *Journal of Clinical Immunology*, *12*(1), 1–10.

31. Rheinländer, A., Schraven, B., & Bommhardt, U. 2018. CD45 in human physiology and clinical medicine. *Immunology Letters*, *196*, 22–32.

32. Altin, J. G., & Sloan, E. K. 1997. The role of CD45 and CD45-associated molecules in T cell activation. *Immunology and Cell Biology*, *75*(5), 430–445.

33. Huntington, N. D., Xu, Y., Puthalakath, H., Light, A., Willis, S. N., Strasser, A., & Tarlinton, D. M. 2005. CD45 links the B cell receptor with cell survival and is required for the persistence of germinal centers. *Nature Immunology*, *7*(2), 190–198.

34. Scholzen, T., & Gerdes, J. 2000. The Ki-67 protein: From the known and the unknown. *Journal of Cellular Physiology*, *182*(3), 311–322.

35. Khodaeiani, E., Fakhrjou, A., Amirnia, M., Babaei-Nezhad, S., Taghvamanesh, F., Razzagh-Karimi, E., & Alikhah, H. 2013. Immunohistochemical evaluation of p53 and Ki67 expression in skin epithelial tumors. *Indian journal of dermatology*, *58*(3), 181–187.

36. Otrock, Z., Mahfouz, R., Makarem, J., & Shamseddine, A. 2007. Understanding the biology of angiogenesis: Review of the most important molecular mechanisms. *Blood Cells, Molecules, and Diseases*, *39*(2), 212–220.

37. Bielenberg, D. R., Bucana, C. D., Sanchez, R., Donawho, C. K., Kripke, M. L., & Fidler, I. J. 1998. Molecular Regulation of UVB-Induced Cutaneous Angiogenesis. *Journal of Investigative Dermatology*, *111*(5), 864–872.

38. Holmes, D. I., & Zachary, I. 2005. The vascular endothelial growth factor (VEGF) family: angiogenic factors in health and disease. *Genome biology*, *6*(2), 209.

39. Sage, H., Vernon, R. B., Funk, S. E., Everitt, E. A., & Angello, J. 1989. SPARC, a secreted protein associated with cellular proliferation, inhibits cell spreading in vitro and exhibits Ca 2-dependent binding to the extracellular matrix. *The Journal of Cell Biology*, *109*(1), 341–356.

40. Chlenski, A., Guerrero, L. J., Peddinti, R., Spitz, J. A., Leonhardt, P. T., Yang, Q., Tian, Y., Salwen, H. R., & Cohn, S. L. 2010. Anti-angiogenic SPARC peptides inhibit progression of neuroblastoma tumors. *Molecular cancer*, *9*, 138.

41. Ledda, M. F., Adris, S., Bravo, A. I., Kairiyama, C., Bover, L., Chernajovsky, Y., … Podhajcer, O. L. 1997. Suppression of SPARC expression by antisense RNA abrogates the tumorigenicity of human melanoma cells. *Nature Medicine*, *3*(2), 171–176. doi: 10.1038/nm0297-171

42. Dejeans, N., Pluquet, O., Lhomond, S., Grise, F., Bouchecareilh, M., Juin, A., … Chevet, E. 2012. Autocrine control of glioma cells adhesion and migration through IRE1 - mediated cleavage of SPARC mRNA. *Journal of Cell Science*, *125*(18), 4278–4287.

43. Chen, X., Iliopoulos, D., Zhang, Q., Tang, Q., Greenblatt, M. B., Hatziapostolou, M., Lim, E., Tam, W. L., Ni, M., Chen, Y., Mai, J., Shen, H., Hu, D. Z., Adoro, S., Hu, B., Song, M., Tan, C., Landis, M. D., Ferrari, M., Shin, S. J., … Glimcher, L. H. 2014. XBP1 promotes triple-negative breast cancer by controlling the HIF1α pathway. *Nature*, *508*(7494), 103–107.

ACADEMIC VITA

Stephen Worrell

EDUCATION

Pennsylvania State University - Schreyer's Honors College
Bachelor of Science, Immunology and Infectious Disease Spring 2020

RELEVANT COURSEWORK

Principles of Immunology	Biology of Function and Development
The Immune System and Disease	Mammalian Physiology
Immunotoxicology of Drugs and Chemicals	Biochemistry 1/2
Biology of Molecules and Cells	Histology
Organic Chemistry 1/2 (+Lab)	Biostatistics
Molecular Pharmacology	Pathobiology (graduate level)
Bacterial Pathogenesis	Current Topics in Immunology

RESEARCH

Pennsylvania State University August 2017- May 2020
Undergraduate Researcher – Glick Lab

- Investigated ER stress response related to mutant Ras driven skin and lung cancers
- Explored role of IRE1alpha in acute and chronic UVB exposure
- Generated Ras-expressing lentivirus used for transduction and oncogenic transformation of cultured primary keratinocytes
- Aided in gamma delta T-Cell immunophenotyping of doxycycline inducible squamous and basal cell carcinoma murine models
- 4 poster presentation based on this work (2x PSU Cancer day, 2x PSU Undergraduate Research Exposition)

Drexel University - College of Medicine Summer 2018
Summer Undergraduate Research Fellowship (SURF) - Nonnemacher Lab

- Utilized CRISPR/Cas-9 gene editing to excise HIV-1 provirus
- Generated CRISPR/Cas-9 lentivirus
- Achieved 98% HIV-1 reduction *in-vitro* using CRISPR/Cas-9 compared to mock treatment
- Formal research presentation and 1 poster presentation (Drexel Discovery day) done based on this work

TECHNICAL SKILLS

- IACUC certified to work with mice. Responsible for hands-on maintenance of large transgenic mouse vivarium (Glick Lab) – skilled in polymerase chain reaction (PCR) for genotyping purposes

- Hands-on experience in flow cytometry (BD LSR Fortessa), Western Blotting, immunohistochemistry (IHC), immunofluorescence (IF), ELISA, quantitative real-time PCR (qRT-PCR), CRISPR/Cas-9 gene editing using lentiviral vectors, mammalian and tumor cell culture

WORK EXPERIENCE

Lion Tutors LLC, State College, PA — February 2017- October 2018

Tutor – Science Department

- Led private introductory biology tutoring
- Assisted in creation of tutoring materials such as review packets, sample exams etc.

VOLUNTEERING

Mount Nittany Medical Center State College, PA — August 2018 – May 2020

Volunteer – Patient Floors

- Aid healthcare professionals with patient care, and lead volunteer training exercises

AWARDS

1. *Agricultural Science Undergraduate Research Award* (Spring 2018, Fall 2019, Spring 2020)
2. *Erickson Discovery Grant*
3. *Poorbaugh Family Scholarship*
4. *Dowler Family Scholarship*
5. *SURF Fellow*
6. *Schreyer Honors Scholar*
7. *Smith Scholarship in Agricultural Science*
8. *Dean's List (7/7 semesters)*